M&C 2017 - International Conference on Mathematics & Computational Methods Applied to Nuclear Science & Engineering, Jeju, Korea, April 16-20, 2017, on USB (2017)

Discontinuity Factors for 1D P_N Equations using a Finite Element Method

A. Vidal-Ferràndiz*, S. González-Pintor†, D. Ginestar‡, G. Verdú*, C. Demazière♮

* *Instituto de Seguridad Industrial: Radiofísica y Medioambiental, Universitat Politècnica de València, 46022, València, Spain*
† *Department of Mathematical Sciences, Chalmers University of Technology, 41296 Göteborg, Sweden*
‡ *Instituto Universitario de Matemática Multidisciplinar, Universitat Politècnica de València, 46022, València, Spain*
♮ *Subatomic and Plasma Physics, Department of Physics, Chalmers University of Technology, 41296 Göteborg, Sweden*
anvifer2@upv.es, sebgonz@chalmers.se, dginesta@mat.upv.es, gverdu@iqn.upv.es, demaz@chalmers.se

Abstract - *The neutron transport equation describes the distribution of neutrons inside a nuclear reactor core. Homogenization strategies have been used for decades to reduce the spatial and angular domain complexity of a nuclear reactor by replacing previously calculated heterogeneous subdomains by homogeneous ones and using a low order transport approximation to solve the new problem. The generalized equivalence theory for homogenization defines discontinuity factors at the boundaries of the homogenized subdomains. In this work, the generalized equivalence theory is extended to the P_N equations for one-dimensional geometries using the finite element method. Here, pin discontinuity factors are proposed instead of the usual assembly discontinuity factors and the use of the spherical harmonics approximation as an extension of the diffusion theory. An interior penalty finite element method is used to discretize and solve the problem using discontinuity factors. Numerical results show that the proposed pin discontinuity factors produce more accurate results than the usual assembly discontinuity factors. The proposed pin discontinuity factors produce precise results for both pin and assembly averaged values without using advanced reconstruction methods. The homogenization methodology is also verified with the calculation of reference discontinuity factors.*

I. INTRODUCTION

Spatial homogenization techniques are applied in different engineering fields for the calculation of complicated systems, comprising numerous heterogeneous components. The main idea of spatial homogenization is to replace heterogeneous subdomains in the reactor core by homogeneous ones so that the homogenized system provides accurate results on such piece-wise homogeneous regions. In nuclear engineering, homogenization is a key method because the large number of components that compose a reactor makes a direct and accurate neutronic calculation computationally unfeasible.

Different homogenization strategies have been developed in the literature. The generalized equivalence theory [1] introduces flux Discontinuity Factors (DFs) to preserve node averaged reaction rates, surface-averaged net currents and the multiplicative factor of the reactor, which is implicitly conserved if the two aforementioned quantities are preserved. Flux discontinuity factors in diffusion theory impose a discontinuity of the neutronic flux in the interior faces of the homogenized regions. On the other hand, the super equivalence homogenization [2] is based on the conservation of pin averaged reactions rates with a correction factor inserted within the cross sections. Finally, the black box homogenization [3] preserves average reaction rates and average reference partial currents through the introduction of current discontinuity factors.

The neutron diffusion equation has been widely used as a low order angular operator for whole core calculations, while the homogenized regions were assemblies. With increasing computational resources available, the homogenized regions have been reduced to the size of a pin. Correspondingly, the angular dependence of the low order operator has to be increased to take into account some transport effects that occur at these smaller scales. For instance one could use the P_N approximation for lower values of N, or the Simplified P_N equations for multidimensional geometries [4, 5].

In this work, we focus on the implementation of the DFs of the generalized equivalence theory for the correction of the homogenization error within a finite element method (FEM), when using P_N equations as low order operator for pin-wise homogenization in one-dimensional geometries. In order to introduce discontinuity factors in the finite element method an Interior Penalty method is used (IP-FEM) [6]. We also present a comparison between assembly-wise and pin-wise homogenizations for different spherical harmonics orders.

The rest of the paper is organized as follows. The one dimensional P_N equations are presented in Section II. These equations are the basis for the multidimensional Simplified P_N equations. Next, we introduce discontinuity factors, including Assembly Discontinuity Factors (ADFs), Pin Discontinuity Factors (PDFs) and Reference Discontinuity Factors (RDFs) in Section III. The Finite Element Method used to discretize the problem which allows the use of discontinuity factors is explained in Section IV. Numerical results for a one-dimensional benchmark are studied in Section V. Finally, the main conclusions of the work are included in Section VI.

II. ONE-DIMENSIONAL P_N EQUATIONS

We consider the eigenvalue problem associated with the multi-group, steady-state, neutron transport equation in slab geometry [7],

$$\left(\mu\frac{\mathrm{d}}{\mathrm{d}x}+\Sigma_t^g(x)\right)\psi^g(x,\mu)=\sum_{g'=1}^{G}\int_{-1}^{1}\Sigma_s^{gg'}(x,\mu_0)\psi^{g'}(x,\mu')\mathrm{d}\mu' + \frac{1}{k_{\mathrm{eff}}}\sum_{g'=1}^{G}\frac{\chi^g(x)}{2}\nu\Sigma_f^{g'}(x)\int_{-1}^{1}\psi^{g'}(x,\mu')\mathrm{d}\mu', \quad (1)$$
$$g=1,\ldots,G, \qquad x\in[0,\,L_t]$$

where G is the number of energy groups considered, θ is the angle between the direction of travel of the neutron and the x axis, $\mu = cos(\theta)$, θ_0 is the change of directions due to scattering collisions, $\mu_0 = cos(\theta_0)$. $\Sigma_t^g(x)$, $\nu\Sigma_f^g(x)$, $\Sigma_s^{gg'}(x,\mu_0)$ are the total, production and scattering cross sections for energy group g, and $\chi^g(x)$ is the fission spectrum. The dominant eigenvalue of the problem (1), k_{eff}, is the multiplicative factor of the system and measures its criticality. The corresponding eigenvector, $\psi^g(x,\mu)$, is the stationary angular flux distribution in the reactor.

The spherical harmonics approximation to the neutron transport equation in slab geometry assumes that the angular dependence of both the neutron flux distribution and the scattering cross-section can be expanded in terms of $N+1$ Legendre polynomials,

$$\psi^g(x,\mu)=\sum_{n=0}^{N}\frac{2n+1}{2}\phi_n^g(x)\,P_n(\mu)\,, \quad (2)$$

$$\Sigma_s^{gg'}(x,\mu_0)=\sum_{n=0}^{N}\frac{2n+1}{2}\Sigma_{sn}^{gg'}(x)\,P_n(\mu_0)\,. \quad (3)$$

Inserting equations (2) and (3) in equation (1), the P_N equations can be expressed in matrix notation [8] as

$$\frac{\mathrm{d}\,\Phi_1}{\mathrm{d}x}+\mathbf{\Sigma_0}\Phi_0=\frac{1}{k_{\mathrm{eff}}}\mathbf{F}\Phi_0\,, \quad (4)$$

$$\frac{\mathrm{d}}{\mathrm{d}x}\left(\frac{n}{2n+1}\Phi_{n-1}+\frac{n+1}{2n+1}\Phi_{n+1}\right)+\mathbf{\Sigma_n}\Phi_n=0\,, \quad (5)$$
$$\text{for } n=1,\,....,\,N\,,$$

where,

$$\mathbf{\Sigma_n}=\begin{pmatrix}\Sigma_t^0-\Sigma_{sn}^{00} & -\Sigma_{sn}^{01} & \ldots & -\Sigma_{sn}^{0G}\\ \vdots & \vdots & \ddots & \vdots\\ -\Sigma_{sn}^{G0} & -\Sigma_{sn}^{G0} & \ldots & \Sigma_t^G-\Sigma_{sn}^{GG}\end{pmatrix},$$

$$\mathbf{F}=\begin{pmatrix}\chi^0\nu\Sigma_f^0 & \chi^0\nu\Sigma_f^1 & \ldots & \chi^0\nu\Sigma_f^G\\ \vdots & \vdots & \ddots & \vdots\\ \chi^G\nu\Sigma_f^0 & \chi^G\nu\Sigma_f^1 & \ldots & \chi^G\nu\Sigma_f^G\end{pmatrix},\quad \Phi_n=\begin{pmatrix}\phi_n^1\\ \vdots\\ \phi_n^G\end{pmatrix}.$$

It must be noted that in many nuclear applications, as usual static reactor calculations, the scattering cross section, Σ_s, is supposed isotropic [8]. Thus, $\mathbf{\Sigma_n}$ is a diagonal matrix for $n > 0$.

Using a linear change of variables, equations (4) and (5) can be expressed as a system of second order elliptic diffusive-like equation for the even moments. For example, the set of P_5 equations is expressed as

$$-\frac{\mathrm{d}}{\mathrm{d}x}\left(\mathbf{D}\frac{\mathrm{d}}{\mathrm{d}x}U\right)+\mathbf{A}U=\frac{1}{k_{\mathrm{eff}}}\mathbf{M}U\,, \quad (6)$$

where the effective diffusion matrix, $\mathbf{D}$, the absorption matrix, $\mathbf{A}$, and the fission matrix, $\mathbf{M}$, are given by

$$\mathbf{D}=\begin{pmatrix}\frac{1}{3}\mathbf{\Sigma_1}^{-1} & 0 & 0\\ 0 & \frac{1}{5}\mathbf{\Sigma_3}^{-1} & 0\\ 0 & 0 & \frac{1}{7}\mathbf{\Sigma_5}^{-1}\end{pmatrix},$$

$$A_{ij}=\sum_{m=1}^{3}\mathbf{c_{ij}^{(m)}}\mathbf{\Sigma_m}\,,\quad M_{ij}=\mathbf{c_{ij}^{(1)}}\mathbf{F}\,,$$

and the following linear change of variables has been applied,

$$U=\begin{pmatrix}u_0\\ u_2\\ u_4\end{pmatrix}=\begin{pmatrix}\Phi_0+2\Phi_2\\ 3\Phi_0+4\Phi_2\\ 5\Phi_0+6\Phi_2\end{pmatrix}. \quad (7)$$

Finally, the coefficients matrix, $\mathbf{c^{(m)}}$ is defined as,

$$\mathbf{c^{(1)}}=\begin{pmatrix}1 & -\frac{2}{3} & \frac{8}{15}\\ -\frac{2}{3} & \frac{4}{9} & -\frac{16}{45}\\ -\frac{8}{15} & -\frac{16}{45} & \frac{64}{225}\end{pmatrix},$$

$$\mathbf{c^{(2)}}=\begin{pmatrix}0 & 0 & 0\\ 0 & \frac{5}{9} & -\frac{4}{9}\\ 0 & -\frac{4}{9} & \frac{16}{45}\end{pmatrix}, \quad (8)$$

$$\mathbf{c^{(3)}}=\begin{pmatrix}0 & 0 & 0\\ 0 & 0 & 0\\ 0 & 0 & \frac{9}{25}\end{pmatrix}.$$

For multidimensional problems the Simplified P_N approximation is obtained substituting the x derivatives by the corresponding two- or three-dimensional gradient operator in equation (6). These equations are much simpler than the multidimensional P_N equations and can be easily implemented using numerical methods suited for diffusion-like equations.

1. Boundary conditions for P_N equations

Here, we study how to introduce vacuum and reflective boundary conditions in the P_N approximation for one-dimensional geometries.

To approximate the vacuum boundary conditions, we shall consider Marshak's conditions [7]. These boundary conditions

impose a restriction on the flux odd moments at each boundary, x_B, given by

$$\int_{\mu_{in}} P_n(\mu)\,\psi^g(x_B,\,\mu)\,\mathrm{d}\mu = 0, \qquad (9)$$
$$\text{for} \quad g = 1,\,2,\,\ldots,\,G, \qquad n = 1,\,3,\,\ldots,\,N.$$

Expanding $\psi(x_B,\mu)$ using equation (2),

$$\int_{\mu_{in}} P_n(\mu)\sum_{n'=0}^{N}\frac{2n'+1}{2}\phi^g_{n'}(x_B,\,\mu)P_{n'}(\mu)\,\mathrm{d}\mu = 0, \qquad (10)$$
$$\text{for} \quad g = 1,\,2,\,\ldots,\,G, \qquad n = 1,\,3,\,\ldots,\,N.$$

Using the orthogonality relation for Legendre polynomials, the Marshak's boundary condition for P_5 equations are

$$\begin{aligned}\frac{1}{2}\Phi_0 + \frac{5}{8}\Phi_2 - \frac{3}{16}\Phi_4 &= -\Phi_1,\\ -\frac{1}{8}\Phi_0 + \frac{5}{8}\Phi_2 - \frac{81}{128}\Phi_4 &= -\Phi_3,\\ \frac{1}{16}\Phi_0 - \frac{25}{128}\Phi_2 - \frac{81}{128}\Phi_4 &= -\Phi_5\,.\end{aligned}$$

Applying the change of variables given by equation (7), the vacuum condition in the P_5 approximation can be applied as

$$-\hat{n}\,\mathbf{D}\frac{\mathrm{d}}{\mathrm{d}x}U(x_B) = \mathbf{B}U(x_B)\,, \qquad (11)$$

where matrix $\mathbf{B}$ is given by the Kronecker product of matrix $\mathbf{b}$ by an $(G\times G)$ identity matrix,

$$\mathbf{B} = \mathbf{b}\otimes\mathbf{I}_{(G\times G)}\,, \qquad \mathbf{b} = \begin{pmatrix} \frac{1}{2} & -\frac{1}{8} & \frac{1}{16} \\ -\frac{1}{8} & \frac{7}{24} & -\frac{41}{384} \\ \frac{1}{16} & -\frac{41}{384} & \frac{407}{1920} \end{pmatrix}, \qquad (12)$$

and $\hat{n}$ is the normal direction of the boundary, either 1 or -1 in one dimensional geometries.

On the other hand, reflective boundary conditions are imposed if all the flux odd moments are set to zero.

$$\phi^g_n(x_B) = 0, \qquad g = 1,\,2,\,\ldots,\,G, \quad n = 1,\,3,\,\ldots,\,N\,. \quad (13)$$

and, reflective boundary conditions are set imposing,

$$\frac{\mathrm{d}}{\mathrm{d}x}u^g_n(x_B) = 0, \qquad g = 1,2,\ldots,G, \quad n = 0,2,\ldots,N\,. \quad (14)$$

These treatments yield to $(N+1)/2$ equations in the boundary that effectively closes the system. We note that both of these boundary conditions treatments contain asymmetric components when N is even. Thus, only odd sets of P_N equations are considered. It must be noted that for each group the P_N system of equations (6) is symmetric because the coefficients $\mathbf{c^{(m)}}$ and $\mathbf{b}$ are symmetric.

III. HOMOGENIZATION METHOD

In the generalized equivalence theory [1], flux discontinuity factors in the diffusion theory are introduced. From now on, we do not explicit the energy dependence to simplify the notation. Thus, given an edge limiting two adjacent homogenized regions, e, the DFs are defined as interface constants f_e^- and f_e^+, such that the scalar flux, ϕ_0, satisfies the following condition

$$f_e^-\phi_0^{h-}(e) = f_e^+\phi_0^{h+}(e)\,, \qquad (15)$$

where ϕ^{h-} and ϕ^{h+} are the lateral limits of the homogenized flux in the interface, $-$ for the left limit and + for the right limit of the homogenized region. Thus, a definition of the discontinuity factors is

$$f_e^- = \frac{\phi_0^-(e)}{\phi_0^{h-}(e)}\,, \qquad f_e^+ = \frac{\phi_0^+(e)}{\phi_0^{h+}(e)}\,, \qquad (16)$$

enforcing continuity for the heterogeneous reconstructed flux [1].

The angular flux in one-dimensional geometries, $\psi(x,\mu)$, can be reconstructed with the different angular moments, ϕ_n, defined in the P_N approximation. Then, an homogeneous problem must be solved in the homogenized subdomain using odd reference flux moments as boundary conditions to calculate the homogeneous even flux moments, in a similar way as the currents are used as boundary conditions for the scalar flux in the neutron diffusion equation. To calculate the discontinuity factors for the P_N equations, equation (16) can be extended to

$$f^+_{n,e} = \frac{u_n^+(e)}{u_n^{h+}(e)}\,, \quad f^-_{n,e} = \frac{u_n^-(e)}{u_n^{h-}(e)}\,, \quad \text{for } n = 0,\,2,\,\ldots,\,N-1\,, \qquad (17)$$

where u_n^- and u_n^+ are the values at left and right extremes of the heterogeneous flux moments extracted from the transport solution and u_n^{h-} and u_n^{h+} are the left and right values of the homogeneous flux moments calculated with the P_N approximation in the homogenized region. Thus, for a given node e shared by two adjacent homogenized subdomains, we have the relationship

$$f^-_{n,e}\,u_n^{h-}(e) = f^+_{n,e}\,u_n^{h+}(e)\,, \quad \text{for } n = 0,\,2,\,\ldots,\,N-1\,. \quad (18)$$

At this point, we need the value of the heterogeneous and homogeneous flux moments, $u(x)$, and $u^h(x)$, respectively, to generate the homogenized cross sections and the discontinuity factors. Since the full heterogeneous solution is not known, the reference values must be determined by calculating each heterogeneous subdomain with the full transport operator. These reference calculations are performed for a *reference problem* [3] whose solution is close enough to the solution that would be obtained if the entire heterogeneous system is calculated. Usually, the reference problem is an isolated assembly with reflective boundary conditions. Then, the assembly homogenized cross sections are generated with assembly heterogeneous flux from the reference problem. The homogeneous flux is the solution of the reference homogeneous assembly with reflective boundary conditions and using the assembly homogenized cross sections. We can calculate

Assembly Discontinuity Factors (ADFs) dividing the heterogeneous flux by the homogeneous flux. A scheme of the problems solved to calculate the ADFs is shown in Fig. 1a. It must be noted that for a homogeneous reflective assembly, as the homogeneous reference problem, the fluxes are spatially constant and all the spherical harmonics expansion terms are zero except the first one. In this work, for homogenization at assembly level, the discontinuity factors for the moments greater than 0 are arbitrarily set to 1.0 .

Another possibility is to use the assembly heterogeneous results to compute pin-wise homogenized parameters. In this way, we solve each homogeneous pin problem using the cross sections and current boundary conditions for the isolated heterogeneous assembly problem. Then, the Pin Discontinuity Factors (PDFs) are calculated by the ratio of the reference pin boundary flux values and the homogeneous problem boundary flux values. This procedure is schematised in Figure 1b.

Finally, the heterogeneous flux calculated for the whole reactor can be used to generate reference cross sections, and appropriate fixed current boundary conditions. With the global k_{eff} and these cross sections, the homogeneous flux can be generated in a particular region considered here as an assembly or a pin. Then, Reference Discontinuity Factors (RDFs) are generated using equation (17). This technique provides exact homogenized parameters, but it requires the solution of the whole heterogeneous problem to generate the homogenized parameters, what makes it of no practical sense. However, it is used here to verify that the homogenization technique is successfully implemented. RDFs strategy corresponds to Fig. 1c.

Moreover, we introduce the concepts of *High Order* (HO) and *Low Order* (LO) operators, meaning that different approximations can be used to solve the equations at different scales, where an HO operator is more accurate to represent space, angle and energy, but more expensive in computational terms. A LO operator has lower accuracy in space, angle and energy, but is computationally less expensive as the P_N approximation in this work. Thus, when we talk about a solution of the original problem, this should be obtained with a HO solver, while the solution of the homogenized problem is obtained by a LO solver. The LO solver for the homogeneous reference problems and for the homogenized problem must be the same, due to the dependence of the discontinuity factors on the LO solver. At least for PDFs and RDFs strategies because for ADFs the fluxes are constant and the method does not matter.

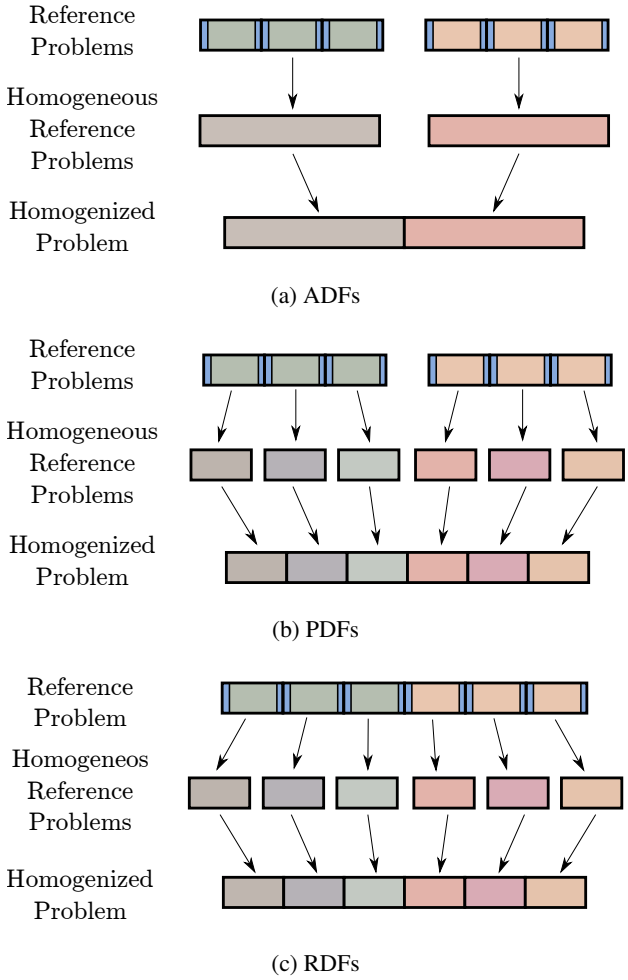

Fig. 1: Homogenization strategies.

IV. FINITE ELEMENT DISCRETIZATION

1. Interior Penalty FEM

For the spatial discretization of the diffusive eigenvalue problem corresponding to equation (6), a Discontinuous Galerkin finite element method is used extending the method presented in [6] for the P_N equations. If discontinuity factors are not taken into account, the interior penalty finite element method can be formulated as follows. First, we choose a partition of the one-dimensional domain, $\mathcal{I}_h$, resulting in a splitting of the original domain defining the reactor, Ω, into subintervals, $I_k = [e_{k-1},\ e_k]$, $k = 1 \ldots, N_k$, defining the mesh. Second, we define $\mathcal{E}_h := \mathcal{E}_h^0 \cup \mathcal{E}_h^\partial$, as the set of all points that define the partition into subintervals, including the boundaries of the domain $\mathcal{E}_h^\partial := \{e_0,\ e_{N_k}\}$, and the interior interfaces $\mathcal{E}_h^0$. Now, problem (6) together with the continuity conditions for the moments and its derivatives, considering homogeneous boundary conditions for clarity, can be rewritten in a generic form, as

$$-\frac{\mathrm{d}}{\mathrm{d}x}\cdot D_n\frac{\mathrm{d}}{\mathrm{d}x}u_n + \Sigma\, u_n = q_n \quad \text{in each } I_k \in \mathcal{I}_h\,, \tag{19}$$

$$[\![u_n(e)]\!] = 0 \quad \text{on each } e \in \mathcal{E}_h\,, \tag{20}$$

$$\left[\!\!\left[D_n\frac{\mathrm{d}}{\mathrm{d}x}u_n(e)\right]\!\!\right] = 0 \quad \text{on each } e \in \mathcal{E}_h^0\,. \tag{21}$$

where the jumps $[\![\cdot]\!]$ are defined by

$$[\![u_n]\!] = \mathbf{n}^- u_n^- + \mathbf{n}^+ u_n^+ = u_n^- - u_n^+,\ \text{on } e \in \mathcal{E}_h^0,$$
$$[\![u_n]\!] = \begin{cases} \mathbf{n}^+ u_n^+(e_0) & = -u_n^+(e_0) \\ \mathbf{n}^- u_n^-(e_{N_k}) & = +u_n^-(e_{N_k}) \end{cases},\ \text{on } e \in \mathcal{E}_h^\partial, \tag{22}$$

where $u_n^{\pm}$ are the lateral limits of u_n in a particular node, and $\mathbf{n}^{\pm}$ are the normal vectors outward to the adjacent cells − and + at the shared node e, so $\mathbf{n}^- = +1$ and $\mathbf{n}^+ = -1$ in one-dimension. The indices for energy group g are avoided for simplicity of the notation, considering all the contributions coming from different energy and moments inside the source term q_n, together with the neutrons produced due to the fission terms. Standard Interior Penalty Finite Element Methods (IP-FEM) exist for the previous problem as follows [9]:

Find $u_n \in \mathrm{H}^1(\mathcal{I}_h)$ such that

$$\left(D_n \frac{\mathrm{d}}{\mathrm{d}x} u_n,\ \frac{\mathrm{d}}{\mathrm{d}x} v\right)_{\mathcal{I}_h} + (\Sigma u_n, v)_{\mathcal{I}_h} - \left(\left\{D_n \frac{\mathrm{d}}{\mathrm{d}x} u_n\right\},\ [\![v]\!]\right)_{\mathcal{E}_h} + (s_1 [\![u_n]\!],\ [\![v]\!])_{\mathcal{E}_h} = (q_n,\ v)_{\mathcal{I}_h},\ \forall v \in \mathrm{H}^1(\mathcal{I}_h)\,, \quad (23)$$

where $\mathrm{H}^1(\mathcal{I}_h) := \left\{v \in \mathrm{L}^2(\Omega) : \quad v_{|I_k} \in \mathrm{H}^1(I_k) \quad \forall I_k \in \mathcal{I}_h\right\}$, s_1 is a penalty parameter large enough to stabilize the problem, the averages $\{\cdot\}$ are defined by

$$\{u\} = \frac{1}{2}(u^- + u^+),\ \text{on } e \in \mathcal{E}_h^0, \quad \{u\} = u,\ \text{on } e \in \mathcal{E}_h^\partial. \quad (24)$$

This problem can be rewritten as: Find $u_n \in \mathrm{H}^1(\mathcal{I}_h)$ such that

$$\left(D_n \frac{\mathrm{d}}{\mathrm{d}x} u_n,\ \frac{\mathrm{d}}{\mathrm{d}x} v\right)_{\mathcal{I}_h} + (\Sigma u_n,\ v)_{\mathcal{I}_h} - \left(\left\{D_n \frac{\mathrm{d}}{\mathrm{d}x} u_n\right\},\ [\![v]\!]\right)_{\mathcal{E}_h^0} + (s_1 [\![u_n]\!],\ [\![v]\!])_{\mathcal{E}_h^0} + D_n(e_0)\frac{\mathrm{d}}{\mathrm{d}x} u_n(e_0) v(e_0) - D_n(e_{N_k})\frac{\mathrm{d}}{\mathrm{d}x} u_n(e_{N_k})\, v(e_{N_k}) = (q_n,\ v)_{\mathcal{I}_h},\ \forall v \in \mathrm{H}^1(\mathcal{I}_h)\,,$$

where we have used the boundary conditions $u(e_0) = 0$ and $u(e_{N_k}) = 0$. We notice that this formulation of the problem is the same as the one obtained in [6] for the neutron diffusion equation with zero flux boundary conditions. For our one-dimensional problem, this notation corresponds to integrals over the elements in $\mathcal{I}_h$ and the evaluation at the elements in $\mathcal{E}_h$ that stands as follows

$$\begin{aligned}
(f,\ g)_{\mathcal{I}_h} &= \sum_{I_k \in \mathcal{I}_h} (f,\ g)_{I_k} = \sum_{I_k \in \mathcal{I}_h} \int_{I_k} f(x) g(x)\, \mathrm{d}x\,,\\
(f,\ g)_{\mathcal{E}_h} &= (f,g)_{\mathcal{E}_h^0} + (f,g)_{\mathcal{E}_h^\partial}\\
(f,\ g)_{\mathcal{E}_h^0} &= \sum_{e \in \mathcal{E}_h^0} (f,\ g)_e = \sum_{e \in \mathcal{E}_h^0} f(e) g(e)\,,\\
(f,\ g)_{\mathcal{E}_h^\partial} &= \sum_{e \in \mathcal{E}_h^\partial} (f,\ g)_e = f(e_0)g(e_0) + f(e_{N_k})g(e_{N_k})\,.
\end{aligned}$$

This formulation is also called Incomplete Interior Penalty Galerkin method (IIPG). A more detailed description of the different operators for higher dimensions can be found in [9]. Different formulations have also been proposed in [10] and [11], where the scheme is consistent with a transport formulation within the strategy of synthetic diffusion acceleration. The inclusion of the discontinuity factors in the finite element method formulation is discussed in the next Section.

2. IP-FEM with discontinuity factors

A scheme to solve equation (6) with discontinuities for the even flux moments has been implemented. This method uses an Interior-Penalty Finite Element Method (IP-FEM) similar to the one developed for diffusion theory presented in [6] and imposes continuity and discontinuity conditions in a weak way by means of redefining the jump operators.

In this case, the reference situation is one assembly or a pin with suitable boundary conditions. Thus, the continuity condition for the flux will be forced to be discontinuous as in equation (18). This type of interface conditions leads to a slightly different problem from the one stated by equations (19), (20) and (21), i.e., the problem with discontinuity factors is of the form

$$-\frac{\mathrm{d}}{\mathrm{d}x} \cdot D_n \frac{\mathrm{d}}{\mathrm{d}x} u_n + \Sigma_n u_n = q_n \quad \text{in each } I_k \in \mathcal{I}_h, \quad (25)$$

$$[\![u_n(e)]\!]_f = 0 \quad \text{on each } e \in \mathcal{E}_h, \quad (26)$$

$$\left[\!\left[D_n \frac{\mathrm{d}}{\mathrm{d}x} u_n(e)\right]\!\right] = 0 \quad \text{on each } e \in \mathcal{E}_h^0. \quad (27)$$

where the new jumps $[\![\cdot]\!]_f$ are defined as follows

$$\begin{aligned}
[\![u_n]\!]_f &= f_{n,e}^- \mathbf{n}^- u_n^- + f_{n,e}^+ \mathbf{n}^+ u_n^+ = f_{n,e}^- u_n^- - f_{n,e}^+ u_n^+,\ \text{on } e \in \mathcal{E}_h^0,\\
[\![u_n]\!]_f &= \begin{cases} f_{n,e_0}^- \mathbf{n}^+ u_n^+(e_0) & = -f_{n,e_0}^- u_n^+(e_0) \\ f_{n,e_{N_k}}^+ \mathbf{n}^- u_n^-(e_{N_k}) & = +f_{n,e_{N_k}}^+ u_n^-(e_{N_k}) \end{cases},\ \text{on } e \in \mathcal{E}_h^\partial,
\end{aligned} \quad (28)$$

where $f_{n,e}^+$ is generally different from $f_{n,e}^-$ for a particular edge e and even moment n, defining the jumps imposed to the solution, u_n. A scheme to approximate the problem defined by equations (25), (26) and (27), has been implemented in an IP-FEM using a formulation based on equation (23) as follows

$$\left(D_n \frac{\mathrm{d}}{\mathrm{d}x} u_n,\ \frac{\mathrm{d}}{\mathrm{d}x} v_n\right)_{\mathcal{I}_h} + (\Sigma_n u_n, v_n)_{\mathcal{I}_h} - \left(\left\{D_n \frac{\mathrm{d}}{\mathrm{d}x} u_n\right\}, [\![v_n]\!]\right)_{\mathcal{E}_h} + \left(s_1 [\![u]\!]_f, [\![v_n]\!]\right)_{\mathcal{E}_h} = (q_n, v_n)_{\mathcal{I}_h}, \quad (29)$$

following analogous steps to the ones presented in [6] for the neutron diffusion equation.

V. NUMERICAL RESULTS

To study the performance of the homogenization method for the P_N equations, a one-dimensional reactor configuration based on the C5G7 benchmark [12] is defined. The benchmark consists of five assemblies of 21.42 cm wide with reflective boundary conditions as Fig. 2 shows. Each assembly is composed of 17 pins of 1.26 cm wide, where each pin is made of nuclear fuel surrounded by a thin layer of water of 0.09 cm. The composition of the assemblies and pins is presented in Fig. 3 and Fig. 4. Seven energy groups cross sections are used in this benchmark as specified in [12]. The transport reference solution is calculated with a discrete ordinates code using a S_{96} approximation where the solution is fully converged.

Fig. 2: Reactor configuration.

The transport reference results are also used to compute reference homogenized cross sections and reference discontinuity factors. The same code is used to compute the isolated assemblies with reflective boundary to calculate assembly-wise and pin-wise homogenized cross sections and discontinuity factors.

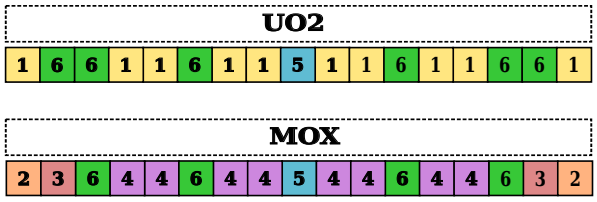

Fig. 3: Assemblies composition.

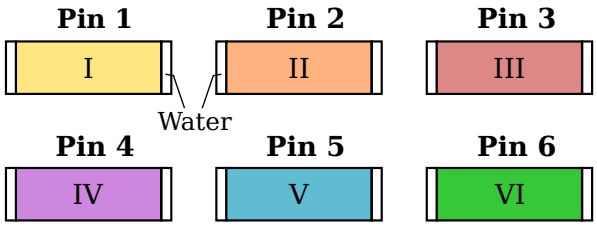

Fig. 4: Pins composition.

First we analyse the behaviour of the fluxes and the errors for different energy groups and different LO solvers (P_1, P_3, and P_5) without spatial homogenization. Fig. 5a and Fig. 5b present the heterogeneous scalar fluxes, ϕ_0^g, of the groups $g = 1$ and $g = 7$ for different transport approximations. Fig. 5c and Fig. 5d show the relative errors for these low order angular approximations. Looking at Fig. 5a for the flux for $g = 1$, and its relative error in Fig. 5c, we see that the error is mostly due to the fact that the lower order approximations P_1, P_3 and P_5 do not capture the local behaviour of the solution in regions with water, where the flux is lower than in fuel regions for fast groups. The same problem occurs when looking at the behaviour for $g = 7$ in Fig. 5b and 5d, but this time because the flux is underestimated in the region with water, where the flux is larger than in regions with fuel for slow groups (high values of g). This behaviour is usual. Moreover, we also observe that the relative error is much bigger for $g = 7$ than for $g = 1$ (about one order of magnitude), but this is mainly due to the fact that the value of the flux is smaller in one order of magnitude, and this means that the absolute value of the error is similar. This effect is enhanced by the fact that strong heterogeneity in the cross sections in the thermal groups ($g > 5$) result in more heterogeneous thermal fluxes as Fig. 5b clearly shows.

Table I shows the assembly and pin averaged errors obtained for the heterogeneous calculation. To compare the results, neutronic power averaged assembly and neutronic power averaged pin errors are condensed using the root mean square of average assembly and pin neutronic power, A-RMS and P-RMS, respectively.

$$\text{RMS} = \sqrt{\frac{1}{L_t}\sum_i L_i \left(\frac{P_i - P_i^*}{P_i^*}\right)^2}\,, \tag{30}$$

where P_i and P_i^* represent the homogeneous and the heterogeneous reference, respectively, averaged neutronic power in the region i. This region can be an assembly for A-RMS or a pin for P-RMS. L_i represents the length of the region i and L_t is the total length of the reactor. In Table I, A-RMS and P-RMS errors are smaller than 2.5%, while the eigenvalue error is above 650 pcm. From these results, it can be seen that low order spherical harmonics approximations cannot reproduce accurately sub-pin heterogeneities and homogenization methods are necessary to improve the results.

P_N	k_{eff}	Δk_{eff} (pcm)	A-RMS (%)	P-RMS (%)
P_1	1.11869	1443	2.05	2.03
P_3	1.12290	1022	1.30	1.17
P_5	1.12649	663	0.75	0.68
Reference $k_{eff} = 1.13312$				

TABLE I: Comparison of heterogeneous results.

Table II shows the results with assembly-wise homogenization for P_1, P_3, P_5 approximations, respectively. We provide the results with volume averaged cross sections and without discontinuity factors (No DFs), then the results using assembly-wise homogenized cross sections with ADFs, and for homogenized cross sections with the true heterogeneous flux together with RDFs for completeness. We can observe that the A-RMS error for the P_1 approximation, equivalent in one dimensional geometries to the diffusion equation, provides accurate results, and that increasing the number of spherical harmonics functions for the angular approximation provides little improvement. This behaviour is explained because the assemblies are large enough to provide accurate average values with diffusion approximation and the angular dependence is not very important. However, the reconstructed pin power results have large P-RMS errors for the pin-wise power distribution, around 15%. This can be explained because of the lack of detailed information about the shape of the function inside the assembly within the whole core homogenized calculation, where the environment is taken into account, thus resulting into inaccurate reconstruction of the pin-wise power distribution. In this work, the pin power reconstruction has been calculated multiplying the assembly averaged power, calculated in homogenized problem, by the pin averaged power, calculated in the reference problem. To improve these results a more sophisticated reconstruction method as [13], [14] or [15] must be used. However these methods are designed for nodal codes and they are not the main object of this work.

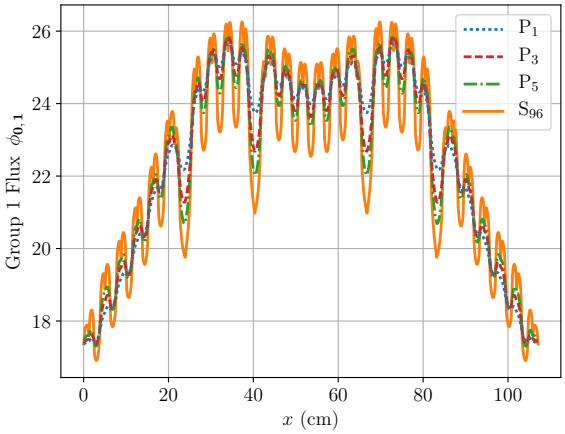

(a) Scalar flux for group 1

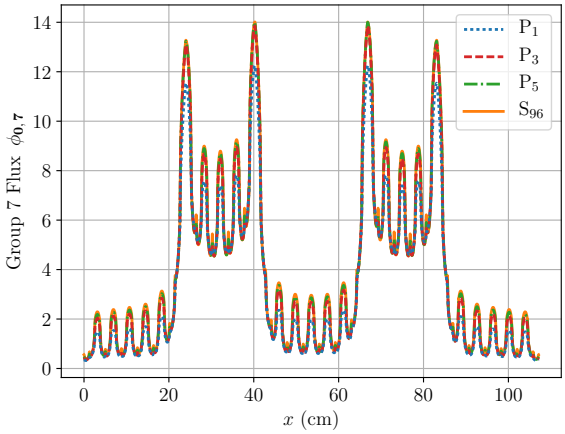

(b) Scalar flux for group 7

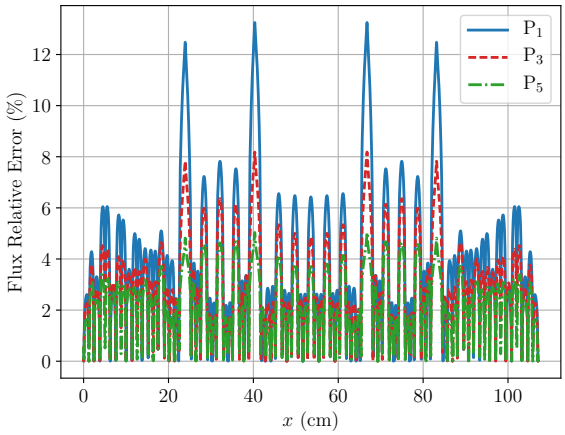

(c) Relative error for group 1

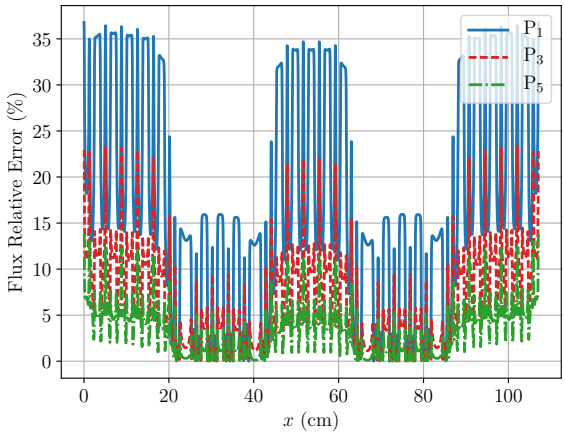

(d) Relative error for group 7

Fig. 5: Comparison of results for heterogeneous fluxes and relative errors.

Table III shows the results with pin-wise homogenization for the same approximations as in the previous Table. They provide more accurate results both in assembly and pin averages, specially if the proposed PDFs are used. More specifically, we can see that the P_1 approximation provides good results and low A-RMS errors, which is not improving by increasing the order of the spherical harmonics approximation. Nevertheless, the improvement of the pin-wise homogenization results in more accurate pin-wise power distributions, where we can observe that higher order for the spherical harmonics approximations results in more accurate pin-wise power distribution, with the P-RMS errors being less than 1% for P_3 and P_5.

The deviation from the reference solution using RDFs with assembly-wise homogenization and pin-wise homogenization are zero, as expected. This is consistent with the idea that having the proper homogenization parameters would allow to exactly reproduce the heterogeneous behavior in the homogenized equations as generalized equivalence theory states [1].

VI. CONCLUSIONS

An extension of the generalized equivalence theory for the one dimensional P_N equations using a finite element method has been developed in this work. This extension proposes accurate Pin Discontinuity Factors for every even flux moment of the spherical harmonics approximation calculated from an isolated assembly transport calculation. An interior penalty finite element method has been presented to discretize and solve the problem using discontinuity factors. Numerical results show that low order spherical harmonics approximations over the heterogeneous composition can be successfully substituted by a two-stage calculation through an homogenization process, resulting in faster calculations. In this way, Assembly Discontinuity Factors produce acceptable eigenvalue and assembly averaged results using diffusion theory

P_N	DFs	k_{eff}	Δk_{eff} (pcm)	A-RMS (%)	P-RMS (%)
P_1	No DFs	1.13462	150	1.20	14.82
	ADFs	1.13334	22	1.52	14.95
	RDFs	1.13312	0	0.00	0.00
P_3	No DFs	1.13613	301	3.54	15.00
	ADFs	1.13392	80	0.95	14.89
	RDFs	1.13312	0	0.00	0.00
P_5	No DFs	1.13618	306	3.55	15.00
	ADFs	1.13398	86	0.94	14.89
	RDFs	1.13312	0	0.00	0.00
Reference k_{eff} = 1.13312					

TABLE II: Results of assembly-wise homogenization.

P_N	DFs	k_{eff}	Δk_{eff} (pcm)	A-RMS (%)	P-RMS (%)
P_1	No DFs	1.12458	854	1.66	1.66
	PDFs	1.13331	19	0.46	1.43
	RDFs	1.13312	0	0.00	0.00
P_3	No DFs	1.12795	517	1.32	1.20
	PDFs	1.13350	55	0.89	0.92
	RDFs	1.13312	0	0.00	0.00
P_5	No DFs	1.13053	259	1.03	0.94
	PDFs	1.13350	38	0.76	0.78
	RDFs	1.13312	0	0.00	0.00
Reference k_{eff} = 1.13312					

TABLE III: Results of pin-wise homogenization.

but they do no reconstruct precise pin averaged results using standard methods. The proposed pin discontinuity factors produce accurate assembly-wise and pin-wise neutron power distributions. Multidimensional extension of this work using the simplified spherical harmonics method will be undertaken in future works.

ACKNOWLEDGEMENTS

The work has been partially supported by the Ministerio de Economía y Competitividad under projects ENE 2014-59442-P and MTM2014-58159-P, the Generalitat Valenciana under PROMETEO II/2014/008 and the Universitat Politècnica de València under FPI-2013. The work has also been supported partially by the Swedish Research Council (VR-Vetenskapsrådet) within a framework grant called DREAM4SAFER, research contract C0467701.

REFERENCES

1. K. SMITH, "Assembly homogenization techniques for light water reactor analysis," *Progress in Nuclear Energy*, **17**, *3*, 303 – 335 (1986).
2. A. HÉBERT and G. MATHONNIERE, "Development of a third-generation superhomogénésation method for the homogenization of a pressurized water reactor assembly," *Nuclear science and engineering*, **115**, *2*, 129–141 (1993).
3. R. SANCHEZ, "Assembly homogenization techniques for core calculations," *Progress in Nuclear Energy*, **51**, *1*, 14–31 (2009).
4. A. YAMAMOTO, T. SAKAMOTO, and T. ENDO, "Discontinuity Factors for Simplified P_3 Theory," *Nuclear Science and Engineering*, **183**, *1*, 39–51 (2016).
5. L. YU, D. LU, and Y. A. CHAO, "The calculation method for SP_3 discontinuity factor and its application," *Annals of Nuclear Energy*, **69**, 14–24 (2014).
6. A. VIDAL-FERRÀNDIZ, S. GONZÁLEZ-PINTOR, D. GINESTAR, G. VERDÚ, M. ASADZADEH, and C. DEMAZIÈRE, "Use of discontinuity factors in high-order finite element methods," *Annals of Nuclear Energy*, **87**, 728–738 (2016).
7. W. M. STACEY, *Nuclear Reactor Physics*, John Wiley & Sons, Weinheim, Germany, 2nd ed. (2007).
8. S. P. HAMILTON and T. M. EVANS, "Efficient solution of the simplified P_N equtations," *Journal of Computational Physics*, **284**, 155–170 (2015).
9. F. BREZZI, B. COCKBURN, L. D. MARINI, and E. SÜLI, "Stabilization mechanisms in discontinuous Galerkin finite element methods," *Computer Methods in Applied Mechanics and Engineering*, **195**, *25*, 3293–3310 (2006).
10. Y. WANG and J. C. RAGUSA, "Diffusion Synthetic Acceleration for High-Order Discontinuous Finite Element SN Transport Schemes and Application to Locally Refined Unstructured Meshes," *Nuclear Science and Engineering*, **166**, *2*, 145–166 (2010).
11. B. TURCKSIN and J. C. RAGUSA, "Discontinuous diffusion synthetic acceleration for Sn transport on 2D arbitrary polygonal meshes," *Journal of Computational Physics*, **274**, 356–369 (2014).
12. E. LEWIS, M. SMITH, N. TSOULFANIDIS, G. PALMIOTTI, T. TAIWO, and R. BLOMQUIST, "Benchmark specification for Deterministic 2-D/3-D MOX fuel assembly transport calculations without spatial homogenization (C5G7 MOX)," Tech. Rep. NEA/NSC/DOC(2001)4, Organization for Economic Cooperation and Development/Nuclear Energy Agency (2001).
13. K. R. REMPE, K. S. SMITH, and A. F. HENRY, "SIMULATE-3 Pin Power Reconstruction: Methodology and Benchmarking," *Nuclear Science and Engineering*, **103**, *4*, 334–342 (1989).
14. T. BAHADIR and S. LINDAHL, "SIMULATE-4 pin power calculations," in "PHYSOR-2006, ANS Topical Meeting on Reactor Physics," Vancuber, BC, Canada (2006), pp. 1–9.
15. H. G. JOO, J. I. YOON, and S. G. BAEK, "Multigroup pin power reconstruction with two-dimensional source expansion and corner flux discontinuity," *Annals of Nuclear Energy*, **36**, *1*, 85–97 (2009).